Rock Mech. Rock Engng. (2001) 34 (4), 275–291

Rock Mechanics and Rock Engineering

Memory Effects in Rock Salt Under Triaxial Stress State and Their Use for Stress Measurement in a Rock Mass

By

Y. L. Filimonov[1], **A. V. Lavrov**[2,3], **Y. M. Shafarenko**[1], and **V. L. Shkuratnik**[2]

[1] Podzemgazprom Ltd., Strength Laboratory, Moscow, Russia
[2] Moscow State Mining University, Physical and Engineering Department, Russia
[3] Present address: Katholieke Universiteit Leuven, Faculty of Applied Sciences, Department of Civil Engineering, Leuven, Belgium

Summary

Regularities of memory effects in rock salt specimens under triaxial stress state were investigated. Each specimen was subjected to two loading cycles. The first cycle was axisymmetric triaxial compression ($\sigma_1 > \sigma_2 = \sigma_3$). The second cycle was uniaxial compression in the direction of σ_1 of the first cycle. Distinct acoustic emission (AE) and deformation memory effects were observed in the second cycle at the stress value equal to a linear combination of the first cycle principal stresses given by $\sigma_1 - (k+1)\sigma_3$, where k is about 0.5–0.6 for rock salt. Anomalies in deformation curves were found to be more reliable than the AE methods in distinguishing memory symptoms. The necessary pre-requisite for memory formation in the first cycle was that σ_1 exceeded the elastic limit, corresponding to the given confining stress σ_3. Inflections in uniaxial stress versus axial strain and lateral strain curves, in the second cycle, were observed at equal stress values if in the first cycle σ_1 exceeded the elastic limit and memory-forming damage was induced. If there was no memory-forming damage, those inflections were seen at different stress values. This characteristic was used to distinguish between true memory effects and natural characteristic points in deformation curves derived from rock salt testing. A new memory symptom was established, namely a turn point in curve "uniaxial stress versus differential coefficient of lateral strains". The results form a basis for application of the memory effects for stress measurement in rock salt masses.

1. Introduction

Predicting and monitoring the stability of structures is of great importance in underground salt mining and construction of underground gas and waste storage caverns in salt. Reliable information on in situ stress state is necessary for the design of the storage caverns as well as for estimation of their stability. At present, overcoring and hydraulic fracturing techniques are normally used for stress measurements. However, both of these methodologies have significant disadvantages, namely high labour-intensity and measurement costs and difficult measurement operation at great depth. These are reasons for increased interest of researchers in

memory properties of rocks, i.e. the ability of rocks to accumulate, to keep and to reproduce information about the stresses which they experienced earlier.

The best studied memory effects are the memory effect in acoustic emission (AE), known as the Kaiser effect, and the deformation memory effects, or memory effects in strains, which make a physical basis of the deformation rate analysis (DRA) stress measurement method. Both kinds of effects take place while the rock is cyclically loaded to stress levels, increasing from cycle to cycle.

The Kaiser effect involves a rapid increase in AE count rate (i.e. number of recorded AE events per time interval), which occurs when the applied stress exceeds the previously applied stress value (the so called pre-stress). At stress values smaller than the pre-stress, AE count rate is close to the background level, or is zero (Kaiser, 1953; Rummel, 1965; Holcomb, 1993; Barr and Hunt, 1999).

The deformation memory effect under cyclic uniaxial loading can be observed as an inflection in the curve "uniaxial compressive stress versus longitudinal (axial) strain" (Shkuratnik and Lavrov, 1997a; Yamshchikov et al., 1994). This inflection takes place when the uniaxial compressive stress reaches its previous peak value.

Both deformation and acoustic emission memory effects are due to the development of irreversible microfractures in rock subjected to cyclic loading (Martin and Chandler, 1994; Eberhardt et al., 1999a). This leads to the absence of crack growth and sliding processes (dislocation movements) at stress values smaller than the maximum previously applied stress. As soon as this "memorized" stress value is attained, crack propagation is again initiated, which is accompanied with AE pulses and non-linear inelastic strain development. These are seen as inflections in strain and AE versus stress curves.

Under uniaxial conditions, both effects can be used for estimation of the maximum previously reached load with a precision acceptable for most practical applications. The measurement error ranges between 5 and 20% (e.g. Kurita and Fujii, 1979; Seto et al., 1997). These promising results were used for developing several new stress measurement techniques (Kuwahara et al., 1990; Yamamoto et al., 1990; Nag et al., 1996; Utagawa et al., 1997; Kudo et al., 1997; Yamamoto et al., 1997; Zhang et al., 1998).

Difficulties arise when reproducing the exact stress state which was acting in situ. An exact restoration of the in situ stress state during laboratory testing would require the knowledge *a priori* of the principal stress ratio as well as the orientation of the principal stress axes in the rock mass. A laboratory test is usually performed in uniaxial compression, assuming the direction to be parallel to the direction of the in situ maximum compressive stress. However, even if the choice of loading direction is correct, the stress states are different in situ as compared to the laboratory. These limitations require further investigation into memory effects during uniaxial loading of rock specimens previously loaded in triaxial compression, as well as the problem of memory manifestation at different stages of triaxial loading.

Experimental studies on the Kaiser effect and the deformation memory effect under triaxial stresses were carried out earlier for various rock types (Holcomb, 1983; Holcomb and Martin, 1985; Panasiyan et al., 1990; Li and Nordlund, 1993; Li, 1998; Momayez and Hassani, 1998). The general procedure for such experiments involves two loading cycles, the first being triaxial loading up to a predefined

stress state followed by uniaxial (or more rarely triaxial) loading up to failure. AE count rate and strains are continuously measured in both loading cycles. Based on these measurements, the first cycle stress value is found at the point where a sharp increase in the AE count rate as well as inflections in the stress-strain curves take place. This stress value is termed the memory effect stress. The procedure described makes it possible to reveal the relationship between principal stress values of the first cycle and the memory effect stress in the second cycle.

Experiments carried out by Momayez and Hassani (1998) have shown that rocks memorize the normal stress component acting in the given direction. Results obtained by Momayez and Hassani (1998) form a basis for the interpretation of stress measurement data as used by several groups of researchers (e.g. Zhang et al., 1998). At the same time, independent experiments performed by Holcomb (1983), Holcomb and Martin (1985), Hughson and Crawford (1987), Li and Nordlund (1993) and Li (1998) have shown that, through triaxial loading, rocks memorize a complex linear combination of principal stresses. When the specimen is reloaded in uniaxial compression (second cycle) in the direction of σ_1 of the first cycle, the Kaiser effect takes place at

$$\sigma_1^{\mathrm{II}} = \sigma_1^{\mathrm{I}} - (k+1)\sigma_3^{\mathrm{I}}, \tag{1}$$

where σ_1^{I} and σ_3^{I} are principal stresses of the first load cycle, k is a dimensionless coefficient, which is individual for each rock, and the index II relates to the second cycle.

In agreement with Eq. (1) is the experimentally established fact that rocks do not memorize uniform hydrostatic compression (Panasiyan et al., 1990; Filimonov et al., 2000).

The experimental result described by expression (1) was later supported by theoretical research. Within the framework of theoretical models developed by Shkuratnik and Lavrov (1995), Lavrov (1997) and Li (1998), k is connected with the coefficient of friction between crack faces in the rock.

The above described problems regarding triaxial stress state are important for all stress measurement methods based on the memory properties of rocks (AE, anelastic strain recovery (ASR), DRA etc.). Investigation of memory regularities in salt is of separate interest because of its unique mechanical behavior. However, despite progress in the utilization of AE-techniques for investigating salt properties and the stress state in salt bodies (Voznesensky et al., 1996; Oxenkrug et al., 1996; Spies and Eisenblätter, 1998; Manthei et al., 1998), the Kaiser effect in salt under triaxial loading is poorly understood. Most works in this field have been carried out under uniaxial loading conditions (Hardy, 1993; Hardy and Shen, 1998). Recent experiments by Filimonov et al. (2000) included two loading cycles, the first of which was hydrostatic compression. The more general case of triaxial axisymmetric pre-loading has not been studied so far.

The objectives of the present work were: a) investigation into memory formation in rock salt at different loading stages (below/above the elastic limit) under triaxial loading conditions b) establishment of a relationship between the stresses to which the rock salt was subjected under triaxial compression (representing the "in situ" state) and the stress value at which memory effects take place when rock

salt is reloaded uniaxially (i.e. the "laboratory test" state); c) establishment of reliable memory indicators for rock salt to be used for in situ stress estimation.

2. Experiment Procedure

The experiments were carried out on specimens of Kaliningrad and Tula rock salt. Kaliningrad rock salt is pure, with an insoluble component of less than 0.5%. The texture is massive, poorly pronounced, layered. The structure is irregularly-grained. The percentage of subidiomorphic coarse-grained halite (3 to 7 mm) in the mass of medium-grained idiomorphic halite (1 to 3 mm) amounts to 10–20%. The microstructure of grains is glassy, rarer poikilitic. Tula rock salt is pure, semi- to non-transparent, with an insoluble component of about 0.5%. The coloration is non-uniform (white halite grains are placed on slightly gray background). The texture is massive, poorly pronounced layered. The structure is irregularly-grained, predominantly coarse-grained. Grains of diameter from 3 to 5 mm and from 0 to 3 mm make 70% and 30%, respectively. The grains are predominantly isometric. Insoluble fine-grained minerals, anhydrite and dolomite, form rare clusters up to 3 mm in diameter, along intergranular contacts. The microstructure of halite grains is glassy, rarer poikilitic.

Testing was performed on eight cylindrically shaped specimens with diameters of 40 mm and lengths of 80 to 90 mm. Where possible, homogeneous salt specimens were used for the testing, avoiding visible macrocracks, cavities, inclusions etc. Although the ISRM recommendations (Brown, 1981) on the specimen diameter with respect to maximum grain size were not always fulfilled, it was believed that careful sample selection helped to reduce the effects of inhomogeneity and grain size. This is supported by the fact that the grain size predominantly effects the crack coalescence stress but not the crack initiation thresholds (Eberhardt et al., 1999b). (Note: the influence of grain size and specimen diameter on memory effects in rock salt and other rock types requires a separate detailed investigation).

The specimens were jacketed in a thin rubber membrane and tested in a triaxial loading cell using a testing machine of type EU-100. Specimens were not removed from the loading cell between the loading cycles. Loading was conducted with a constant axial strain rate of $\dot{\varepsilon}_1 \approx 1.7 \cdot 10^{-5}$ s^{-1}.

During the test of each specimen, the confining pressure (σ_3), the stress difference ($\sigma_1 - \sigma_3$), the axial (ε_1) and lateral (ε_3) strains as well as the AE count rate (N) were automatically measured and recorded using computerized equipment (Fig. 1). The AE signals were measured by a wide-band piezoelectric transducer with a resonant frequency of 200 kHz attached on the upper loading plate (Fig. 1). The pre-amplifier gain was 40 dB and that of the main amplifier integrated in the AE system (AF-15) was 80 dB. The noise threshold of the system was 0.1 V. AE signals were filtered in the frequency range from 20 kHz to 200 kHz (see Voznesensky and Demtchishin, 2000; Voznesensky et al., 1996 for more details).

Two series of specimens were tested using confining pressures ($\sigma_2^{\mathrm{I}} = \sigma_3^{\mathrm{I}}$) of 5 or 10 MPa in the first loading cycle. The loading sequence of each specimen was as follows:

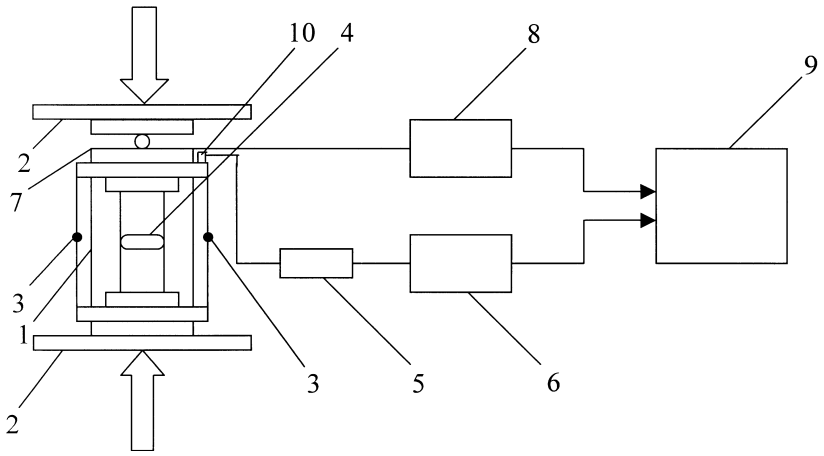

Fig. 1. Schematic diagram of the measurement system: *1* triaxial loading cell; *2* loading platens; *3* strain gauges for axial strain; *4* strain gauges for lateral strain; *5* AE pre-amplifier; *6* AE apparatus (AF-15); *7* load gauge; *8* strain measuring system (SIIT-2); *9* IBM PC with hard disk; *10* AE transducer

1. Increase of the hydrostatic pressure ($\sigma_1 = \sigma_2 = \sigma_3$) on the specimen to 5 MPa (or 10 MPa, as in the case of the second series).
2. Increase of the axial stress (σ_1) while holding the confining pressure (σ_3) constant at 5/10 MPa. Axial stress is increased to the pre-defined maximum value σ_1^{I}, lower than the compressive strength corresponding to the given confining pressure.
3. Decrease the axial stress σ_1 from the maximum value σ_1^{I} down to the hydrostatic stress (5/10 MPa).
4. Remove the hydrostatic pressure from the specimen.
5. Increase in the uniaxial stress up to macrofracture (cycle II).

It should be noted that the axial load during the first cycle (loading step 3) was decreased immediately after it had reached its maximum value σ_1^{I}. Thus, the exposure time to the maximum axial load during the first cycle was approximately zero. The second cycle (loading step 5) was started immediately after unloading of the hydrostatic pressure. The time delay between the two loading cycles was nearly zero (Fig. 2).

On the basis of the measurement data, the following curves were plotted for each specimen: "stress difference ($\sigma_1 - \sigma_3$) versus axial strain (ε_1)", "stress difference ($\sigma_1 - \sigma_3$) versus lateral strain (ε_3)" and "AE count rate versus stress difference ($\sigma_1 - \sigma_3$)". In addition, the volumetric strain $\varepsilon_v = \varepsilon_1 + 2\varepsilon_3$ and the cumulative AE counts were calculated and the curves "stress difference ($\sigma_1 - \sigma_3$) versus volumetric strain (ε_v)" and "cumulative AE counts versus stress difference ($\sigma_1 - \sigma_3$)" were plotted. The values of the stress were corrected for increasing diameter of the specimen.

Note that in the data processing described above, the axial and lateral strains are related to the specimen dimensions before the first loading cycle, l_0^{I} and d_0^{I}. However, when studying the memory effects in rock samples extracted from a rock

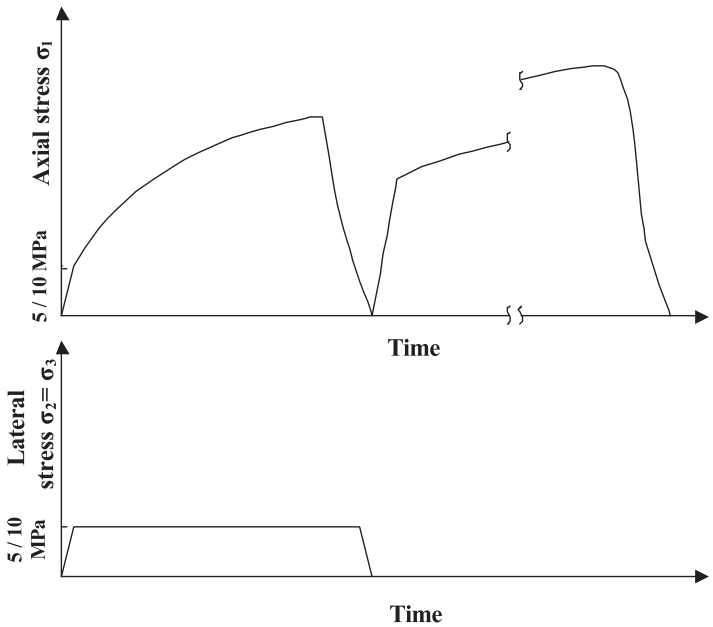

Fig. 2. Axial (σ_1) and lateral ($\sigma_2 = \sigma_3$) stress versus time during both load cycles (schematic plot)

mass with the aim of estimating the in situ state of stress, only the second loading cycle is performed. In this case, the strains are normalized with respect to the specimen dimensions after the first cycle, l_0^{II} and d_0^{II}. That is why "true" strains of the specimens were additionally calculated in the second loading cycle (related to the specimen dimensions before the second cycle, l_0^{II} and d_0^{II}):

$$\varepsilon_1^t = [\varepsilon_1 - (l_0^{\mathrm{II}} - l_0^{\mathrm{I}})/l_0^{\mathrm{I}}]l_0^{\mathrm{I}}/l_0^{\mathrm{II}}, \tag{2}$$

$$\varepsilon_3^t = [\varepsilon_3 - (d_0^{\mathrm{II}} - d_0^{\mathrm{I}})/d_0^{\mathrm{I}}]d_0^{\mathrm{I}}/d_0^{\mathrm{II}}, \tag{3}$$

where l_0^{I}, d_0^{I} and l_0^{II}, d_0^{II} are the specimen dimensions (length, diameter) before the first and the second cycles respectively; ε_1 and ε_3 are the measured axial and lateral strains normalized with respect to the specimen dimensions before the first cycle; ε_1^t and ε_3^t are the strains normalized with respect to the specimen dimensions before the second cycle.

On the basis of the calculated "true" strains ε_1^t and ε_3^t, values of the ratio $\Delta\varepsilon_3^t/\Delta\varepsilon_1^t$ were calculated using the "sliding window" method (see e.g. Eberhardt et al., 1998a), over a window of 50 to 100 data points. These values refer to the center of the sliding window. The scanning step was equal to two points which is in agreement with recommendations given by Eberhardt et al. (1998a).

After the data processing described above, curves "true lateral strain (ε_3^t) versus true axial strain (ε_1^t)" and "the ratio ($\Delta\varepsilon_3^t/\Delta\varepsilon_1^t$) versus stress difference ($\sigma_1 - \sigma_3$)" were plotted for the second loading cycle.

3. Experimental Results

The experiments have shown that the character, the distinctness and even the existence of memory effects in rock salt strongly depend on the deformation stage reached by the specimen in the first cycle. Typical deformation stages of rock salt under triaxial state of stress are illustrated in Fig. 3. Within the interval OA volumetric rock compression occurs due to pore and crack closure. Thereafter, an interval of linear elastic deformation follows (AB). The stress value corresponding to the end of the linear axial deformation is termed the elastic limit σ_{1e} (point B). After exceeding the elastic limit, non-linear deformation begins, and at point C, volumetric strain begins to increase (i.e. dilatancy). For most specimens tested under triaxial conditions the elastic limit was considerably lower than the dilatancy onset stress value σ_{1d} (Fig. 3).

Memory effects are related to irreversible, stress-induced changes in the rock's structure occurring in the first cycle loading (Matsuki and Kojima, 1995; Li, 1998; Lavrov, 1997). Therefore, the elastic limit presents a natural threshold for memory formation. Above σ_{1e}, brittle (cracks) and sliding processes proceed forming the stress memory (Eberhardt et al., 1999a).

This is confirmed by the tests in which the first cycle axial stress was smaller than the elastic limit for the given confining pressure. In this case, no inflections in deformation curves and no bursts or other anomalies in AE were observed in the second cycle. The second cycle deformation and AE curves of such specimens were similar to those of "fresh" samples, which did not undergo any first cycle

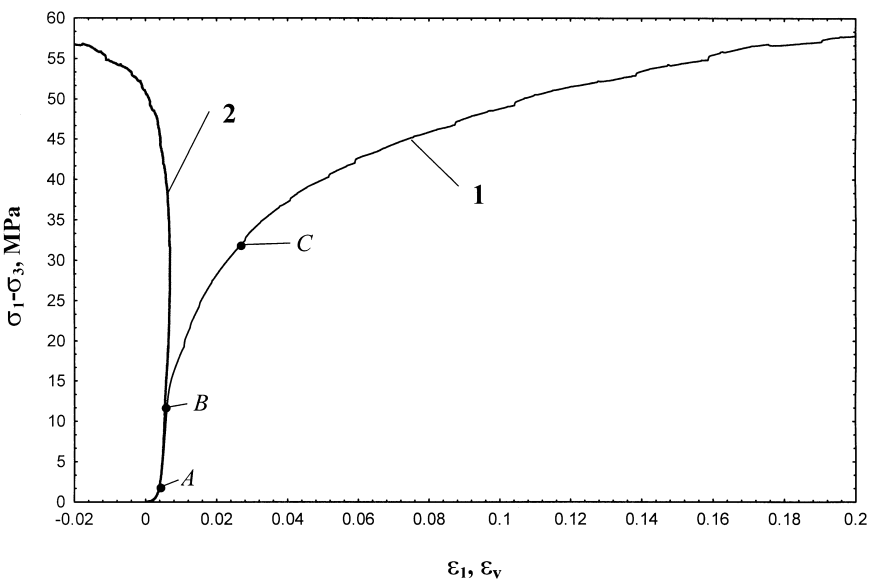

Fig. 3. Axial (ε_1, curve 1) and volumetric (ε_v, curve 2) strains versus stress difference ($\sigma_1 - \sigma_3$) for a single cycle triaxial test performed on a rock salt specimen ($\sigma_2 = \sigma_3 = 10$ MPa): *A* crack and pore closure; *B* elastic limit; *C* onset of dilatancy

loading. This was due to the absence of microfracture damage below the elastic limit which could form a stress memory.

Distinct memory effects in the second cycle take place, if in the first cycle the maximum axial stress exceeded the elastic limit:

$$\sigma_1^{\mathrm{I}} > \sigma_{1e} \tag{4}$$

In this case, there always are distinct inflections in the plots "stress difference $(\sigma_1 - \sigma_3)$ versus axial strain (ε_1)", "stress difference $(\sigma_1 - \sigma_3)$ versus lateral strain (ε_3)" and "stress difference $(\sigma_1 - \sigma_3)$ versus volumetric strain ε_v", during the second cycle. In the curves "$(\sigma_1 - \sigma_3)$ versus ε_1" and "$(\sigma_1 - \sigma_3)$ versus ε_3" the inflection is evident as an abrupt change in the slope of the curve. In the curve "$(\sigma_1 - \sigma_3)$ versus ε_v", the inflexion appears together with a change of the derivative sign (Fig. 4). It

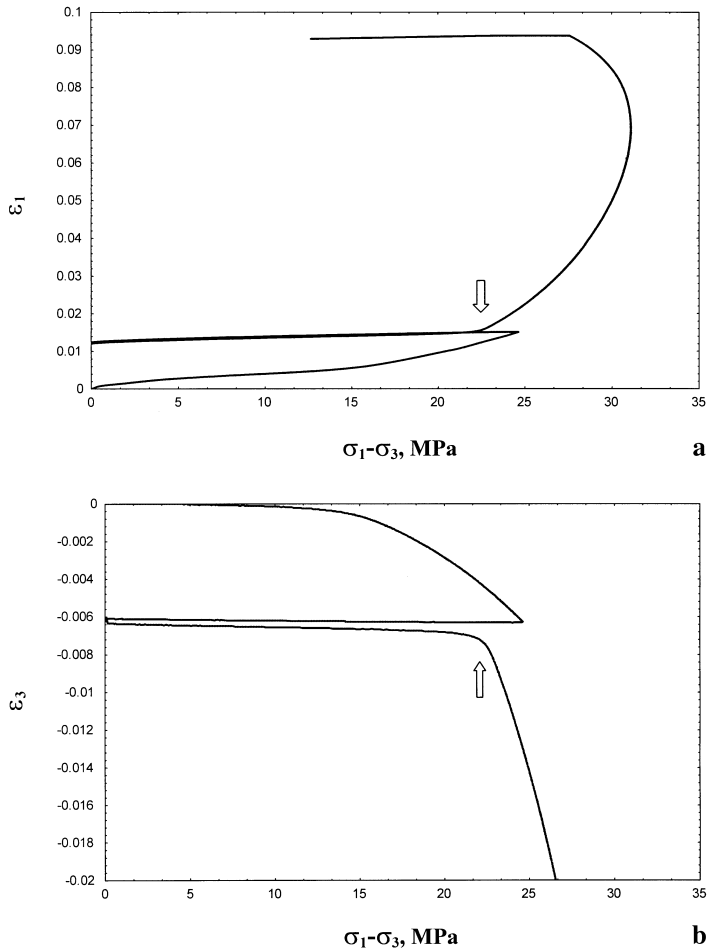

Fig. 4a–c. Axial **(a)**, lateral **(b)** and volumetric **(c)** strains versus stress difference in two successive loading cycles for specimen 3T-119 (where $\sigma_1^{\mathrm{I}} = 30$ MPa and $\sigma_2^{\mathrm{I}} = \sigma_3^{\mathrm{I}} = 5$ MPa in the first cycle). The memory effects in the second cycle take place at $\sigma_1 = 22.5$ MPa as indicated by the arrows

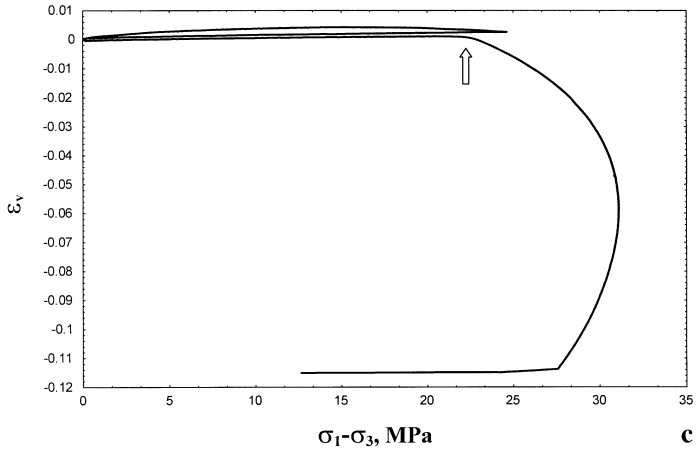

Fig. 4 (continued)

should be noted that in the second cycle the confining pressure is equal to zero. Therefore, σ_1 is written instead of $(\sigma_1 - \sigma_3)$ for the second cycle. The change of the derivative sign in the curve "σ_1 versus ε_v" indicates that the rock compression changes to dilatancy. The stress value at which dilatancy begins in the second cycle, is the same as the stress value at which inflections are seen in curves "σ_1 versus ε_1" and "σ_1 versus ε_3".

Our experiments with salt specimens subjected to various values of σ_1^{I} and σ_3^{I} in the first cycle have shown that the memory effect stress obtained in the second cycle is linked to σ_1^{I} and σ_3^{I} by Eq. (1). The coefficient k ranges between 0.4 and 0.75. It is not improbable that k is dependent on the loading stage of salt. k has an average value of 0.5 to 0.6. Apart from the natural inhomogeneity of the rock salt, the scatter of k can be caused by the sometimes insufficient distinctness of the characteristic anomalies which are interpreted as memory effects. This can introduce an error in the subjective interpretation of the inflections in deformation curves. For practical applications of the memory effects in the future, it is necessary to develop a unified procedure of the data processing with the aim towards more objective identification of the inflections.

A step forward in this direction could be the use of the curve "differential coefficient of lateral strains $(\Delta\varepsilon_3^t/\Delta\varepsilon_1^t)$ versus stress (σ_1)" obtained by the sliding window method (i.e. instead of the curves "σ_1 versus ε_1" and "σ_1 versus ε_3"). In curves "$\Delta\varepsilon_3^t/\Delta\varepsilon_1^t$ versus σ_1", the memory effect is clearly seen as a turn point where the ratio $\Delta\varepsilon_3^t/\Delta\varepsilon_1^t$ abruptly stops to decrease and remains nearly constant as the "memorized" stress value is reached (Fig. 5).

The Kaiser effect is seen in curves "AE count rate versus stress σ_1" as an AE peak (Fig. 6a), if the specimen was loaded over the elastic limit in the first cycle. In addition to the main burst, one or several other bursts can appear (Fig. 6b). In this case, the main burst may not be very distinct, making the recognition of the "memorized" stress level from curves "AE count rate versus stress" more difficult

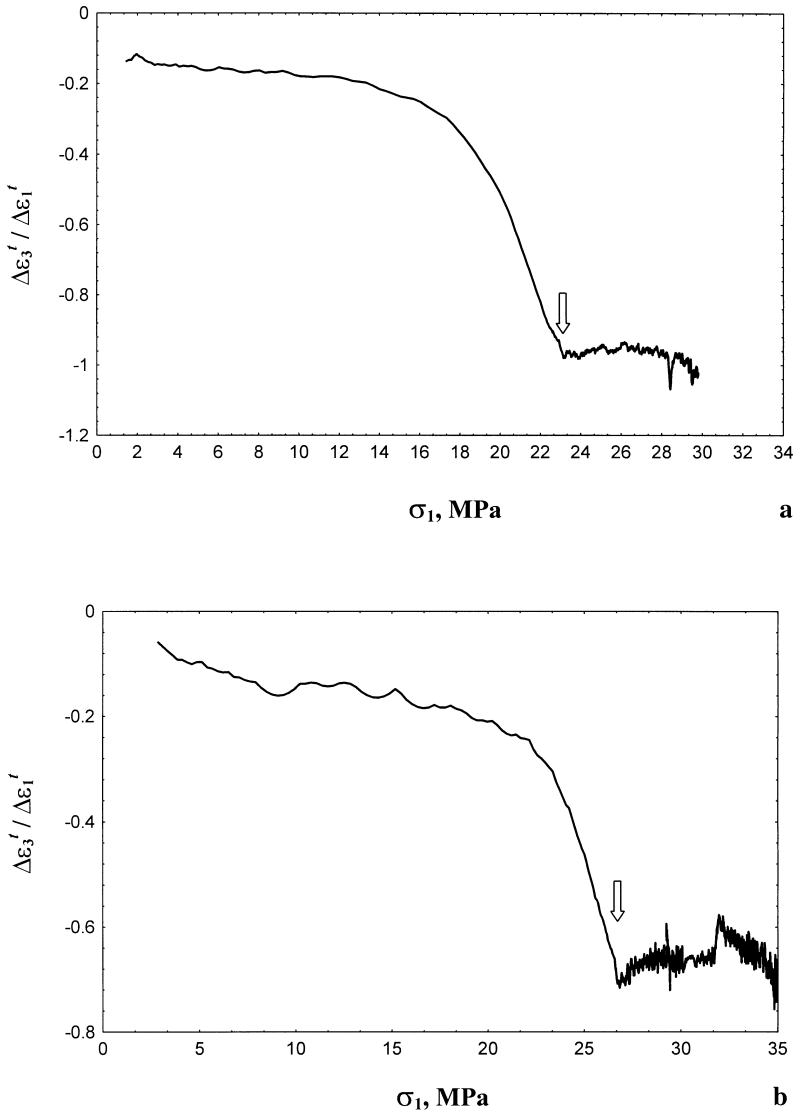

Fig. 5. Ratio of $\Delta\varepsilon_3^t/\Delta\varepsilon_1^t$ versus stress in the second cycle for specimens 3T-119 **(a)** and 3T-141 **(b)**. (Specimen 3T-119 tested with $\sigma_1^{\mathrm{I}} = 30$ MPa and $\sigma_2^{\mathrm{I}} = \sigma_3^{\mathrm{I}} = 5$ MPa; specimen 3T-141 tested with $\sigma_1^{\mathrm{I}} = 35$ MPa and $\sigma_2^{\mathrm{I}} = \sigma_3^{\mathrm{I}} = 5$ MPa). Memory effects are indicated by arrows

than from the deformation curves. The test results thus show that because of the uncertainty and unreliability of the Kaiser effect in rock salt under triaxial state of stress, this effect can only be used as an additional indicator of the recollection of the earlier applied stresses. It is quite possible that there is no detectable Kaiser effect in the specimens whereas there are distinct deformation memory effects.

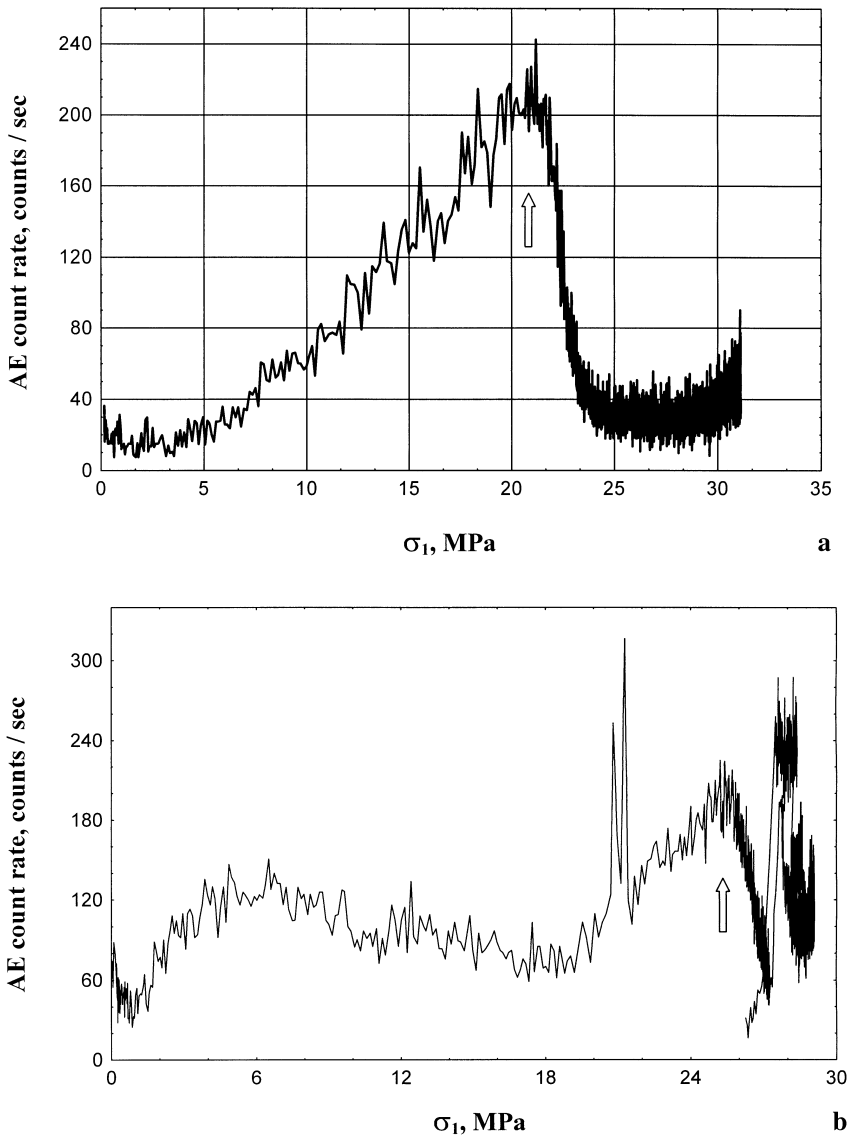

Fig. 6. AE count rate versus stress in the second cycle for specimens 3T-119 **(a)** and 3T-101 **(b)**. Specimen 3T-119 was tested with $\sigma_1^I = 30$ MPa and $\sigma_2^I = \sigma_3^I = 5$. Specimen 3T-101 was tested with $\sigma_1^I = 40$ MPa and $\sigma_2^I = \sigma_3^I = 10$ MPa in the first cycle. Memory effects are indicated by arrows

4. Discussion

Formation of distinct memory effects in the stress range defined by Eq. (4) is explained by intensive crack growth at these stresses. The cracks grow in a stable fashion, i.e. stress increase is required for crack growth. The crack lengths after the first loading cycle are determined by the maximum level of the stress state achieved

in the first cycle (e.g. Nemat-Nasser and Horii, 1982; Dyskin et al., 1999). While being reloaded in the second cycle, a crack starts growing only when the stress exceeds the "memorized" value. The latter is defined by the linear combination of the principal stresses applied in the first cycle (Eq. (1)) as it was theoretically shown by Li (1998), Lavrov (1997), Lavrov and Yasinski (2000).

The complex pattern seen in the curves "AE count rate versus stress" plotted for the second cycle (i.e. the presence of AE from the onset of loading, several bursts and then a subsequent drop in the AE count rate) is in agreement with the results of earlier conducted theoretical research (Lavrov, 1997; Shkuratnik and Lavrov, 1997b; Lavrov, 1998). AE at lower stress values may be due to the initialization of cracks that did not propagate during the first cycle due to the applied confining pressure ($\sigma_2^{\mathrm{I}} = \sigma_3^{\mathrm{I}} = 5/10$ MPa). This is due to the change in the stress state type in the second cycle (i.e. uniaxial) compared with that of the first cycle (i.e. triaxial).

The decrease in the AE count rate after reaching its maximum value (in the form of an AE burst) may be caused by crack intersections as well as by stress shadow effects of neighbouring pores and cracks (Kranz, 1979; Eberhardt et al., 1998b). Approaching macrofracture of the specimen, the AE activity increases again. It seems to be associated with the formation of larger cracks which are parallel to the specimen axis. Such cracks were clearly seen on the surface of the specimens extracted from the loading cell after the completion of the second cycle.

The presence of several characteristic anomalies in AE-curves at stress values below the Kaiser effect stress was also noted by Momayez and Hassani (1998) in their tests involving uniaxial loading of granite samples which were previously subjected to triaxial compression.

The results obtained in the experiments should help to distinguish between the true memory effects in rock salt cores and the familiar inflections related to the elastic limit and to the onset of dilatancy. Namely, if the inflections in curves "stress (σ_1) versus axial strain (ε_1)" and "stress (σ_1) versus lateral strain (ε_3)" take place concurrently and at the same stress value, they indicate the deformation memory effect. An additional memory symptom, although one that was not always observed, can be the Kaiser effect which appears as a local maximum (burst) in the curve "AE count rate versus stress". The Kaiser effect takes place at the same stress as the above mentioned inflections in the deformation curves. This enables one to estimate the in situ principal stress relation given by Eq. (1), with $k = 0.5$–0.6.

If the inflections in curves "σ_1 versus ε_1" and "σ_1 versus ε_3" are seen at different stress values, they do not indicate rock memory on the previously applied stress state, and should be attributed to the elastic limit and the onset of dilatancy, respectively. In both strain curves, the inflections are indistinct, and the Kaiser effect is not observed.

To verify the complex methodology of the data interpretation described above, several specimens of Tula rock salt extracted from 875 m depth were tested in uniaxial compression within a few days after recovery. The short time duration between drilling and testing allowed the assumption that memory did not disappear (Barr and Hunt, 1999; Li and Nordlund, 1993). Specimens were drilled from the Earth surface in vertical direction from a natural bedded salt mass. This direction

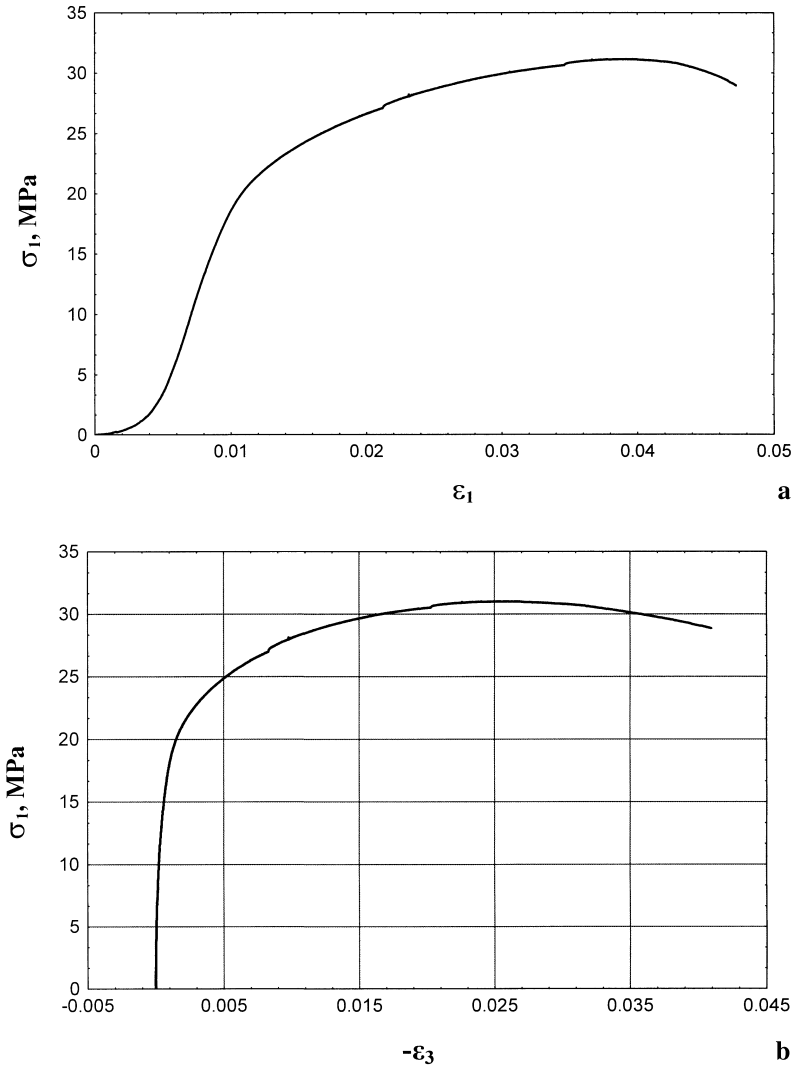

Fig. 7. Axial stress σ_1 versus axial strain **(a)** and lateral strain **(b)** in a uniaxial compression test of a Tula rock salt specimen extracted from the rock mass (875 m depth) 40 hours before the test

was supposed to be parallel to the σ_1-direction in situ. The overburden pressure at the point of extraction is about 20 MPa. The confining stress, given the Poisson's ratio $\nu = 0.3$, is estimated at about 8.5 MPa, and the in situ stress difference is thus 11.5 MPa. This latter value is located within the elastic region of the salt (Fig. 3). Hence, no stress memory was expected in the specimens tested.

This theoretical prediction was proved by the test results. In AE curves, no distinct bursts or other anomalies were observed which could be interpreted as the Kaiser effect. Inflections in curves "σ_1 versus ε_1" and "σ_1 versus ε_3" were indistinct (Fig. 7). No inflections/turn points similar to those described in section 3

were observed in the curves "$\Delta\varepsilon_3^f/\Delta\varepsilon_1^f$ versus σ_1". All deformation curves were rather similar to those obtained in uniaxial tests of rock salt specimens which had been pre-stressed in hydrostatic compression (Filimonov et al., 2000). The test results confirmed the theoretical prediction that in the rock mass in question $(\sigma_1 - \sigma_3)$ does not exceed the elastic limit, i.e. is smaller than 12 MPa.

5. Conclusions

The main conclusions to be drawn from the experiments are as follows:

The necessary condition for stress memory formation in rock salt in the first loading cycle is that the maximum principal stress σ_1 exceeds the elastic limit corresponding to the given confining pressure. If so, the characteristic inflections in the curves "σ_1 versus ε_1", "σ_1 versus ε_3", "$\Delta\varepsilon_3/\Delta\varepsilon_1$ versus σ_1", and AE bursts are distinct and observed at one and the same stress value during the second cycle, which is performed in uniaxial compression. The inflections in strain curves are more reliable memory indicators than the Kaiser effect. The uniaxial stress value at which memory effects are observed in the second cycle, is defined by Eq. (1) where k is about 0.5–0.6 for rock salt.

If rock salt was loaded below the elastic limit in the first cycle, the memory-forming damage was not induced, and the inflections in deformation curves are seen at different stress values in the second cycle, corresponding to natural deformation thresholds (elastic limit and dilatancy onset).

It can be concluded from the experimental results and theoretical background, that the Kaiser effect and DRA techniques can be efficiently used for stress measurement in rock salt only when the maximum in situ principal stress exceeds the elastic limit corresponding to the in situ confining stress.

Uniaxial loading of some recently cored salt specimens has shown that no memory-producing damage was created in natural conditions. This is in agreement with theoretical predictions, according to which the vertical in situ stress did not exceed the elastic limit corresponding to the in situ confining stress.

Acknowledgements

The authors are grateful to Y. S. Oxenkrug, M. N. Tavostin and A. S. Voznesensky for useful discussions and to M. G. Dickert for his help during experiments. Thanks are given to anonymous reviewers whose comments and suggestions helped to considerably improve the manuscript. A. V. Lavrov and V. L. Shkuratnik gratefully acknowledge the support of the Russian Foundation for Basic Research for this work (Project No. 00-15-98590).

References

Barr, S. P., Hunt D. P. (1999): Anelastic strain recovery and the Kaiser effect retention span in the Carnmenellis granite, U.K. Rock Mech. Rock Engng. 32 (3), 169–193.

Brown, E. T. (1981): Rock characterization testing and monitoring: ISRM suggested methods. Pergamon Press, Oxford.

Dyskin, A. V., Germanovich, L. N., Ustinov, K. B. (1999): A 3-D model of wing crack growth and interaction. Engng. Fract. Mech. 63 (1), 81–110.

Eberhardt, E., Stead, D., Stimpson, B., Read, R. S. (1998a): Identifying crack initiation and propagation thresholds in brittle rock. Can. Geotech. J. 35(2), 222–233.

Eberhardt, E., Stead, D., Stimpson, B., Lajtai, E. Z. (1998b): The effect of neighbouring cracks on elliptical crack initiation and propagation in uniaxial and triaxial stress fields. Engng. Fract. Mech. 59 (2), 103–115.

Eberhardt, E., Stead, D., Stimpson, B. (1999a): Quantifying progressive pre-peak brittle fracture damage in rock during uniaxial compression. Int. J. Rock Mech. Min. Sci. 36 (3), 361–380.

Eberhardt, E., Stimpson, B., Stead, D. (1999b): Effects of grain size on the initiation and propagation thresholds of stress-induced brittle fracture. Rock Mech. Rock Engng. 32 (2), 81–99.

Filimonov, Y. L., Lavrov, A. V., Shafarenko, Y. M., Shkuratnik, V. L. (2000): Experimentelle Untersuchung des Steinsalzes mittels einaxialem Drucktest nach hydrostatischer Vorbelastung. Glückauf-Forschungshefte 61 (2), 80–83 (in German).

Hardy, H. R., Jr. (1993): Evaluation of in situ stresses in salt using acoustic emission techniques. In: Proc., 7th Symp. on Salt vol. 1. Elsevier, Amsterdam, 49–58.

Hardy, H. R., Jr., Shen, H. W. (1998): Acoustic emission in salt during elastic and inelastic deformation. In: Proc., 6th Conf. AE/MA in Geologic Structures and Materials. Trans. Tech. Publ., Clausthal-Zellerfeld, 15–28.

Holcomb, D. J. (1983): Using acoustic emission to determine in situ stress: problems and promise. In: Proc., Applied Mechanics, Bioengineering and Fluids Engineering Conference, Houston, 11–21.

Holcomb, D. J. (1993): Observation of the Kaiser effect under multiaxial stress states: implications for its use in determining in situ stress. Geophys. Res. Lett. 20 (19), 2119–2122.

Holcomb, D. J., Martin, R. J. III (1985): Determining peak stress history using acoustic emissions. In: Research and Engineering Applications in Rock Masses. Proc., 26th U.S. Symp. Rock Mech. vol. 2. Balkema, Rotterdam, 715–722.

Hughson, D. R., Crawford, A. M. (1987): Kaiser effect gauging: the influence of confining stress on its response. In: Proc., 6th Int. Congr. Rock Mech. vol. 2. Balkema, Rotterdam, 981–985.

Kaiser, J. (1953): Erkenntnisse und Folgerungen aus der Messung von Geräuschen bei Zugbeanspruchung von metallischen Werkstoffen. Archiv Eisenhüttenwesen 24 (1/2), 43–45.

Kranz, R. L. (1979): Crack-crack and crack-pore interactions in stressed granite. Int. J. Rock Mech. Min. Sci. Geomech. Abstr. 16 (1), 37–47.

Kudo, R., Yokoyama, T., Ito, H., Kuwahara, Y., Nishizawa, O., Yamamoto, K. (1997): Stress measurements with core samples by AE-DRA methods in the 1995 Hyogoken-nanbu earthquake source region. In: Rock Stress. Proc., Int. Symp. on Rock Stress. Balkema, Rotterdam, 359–362.

Kurita, K., Fujii, N. (1979): Stress memory of crystalline rocks in acoustic emission. Geophys. Res. Lett. 6 (1), 9–12.

Kuwahara, Y., Yamamoto, K., Hirasawa, T. (1990): An experimental and theoretical study of inelastic deformation of brittle rocks under cyclic uniaxial loading. Tohoku Geoph. J. (Sci. Rep. Tohoku Univ., Ser. 5) 33 (1), 1–21.

Lavrov, A. V. (1997): Three-dimensional simulation of memory effects in rock samples. In: Rock Stress. Proc., Int. Symp. on Rock Stress. Balkema, Rotterdam, 197–202.

Lavrov, A. V. (1998): Development of theoretical models of emission memory effects in rocks. Ph.D. thesis, Moscow State Mining University, Russia (in Russian).

Lavrov, A. V., Yasinski, M. V. (2000): On the influence of intermediate principal stress upon acoustic emission in cyclically loaded rocks. In: Proc., 10th Session of the Russian Acoustical Society. GEOS, Moscow, 211–214 (in Russian; extended abstract in English at URL: http://www.akin.ru/e_main.htm).

Li, C. (1998): A theory for the Kaiser effect and its potential applications. In: Proc., 6th Conf. AE/MA in Geologic Structures and Materials. Trans. Tech. Publ., Clausthal-Zellerfeld, 171–185.

Li, C., Nordlund, E. (1993): Experimental verification of the Kaiser effect in rocks. Rock Mech. Rock Engng. 26 (4), 333–351.

Manthei, G., Eisenblätter, J., Saltzer, K. (1998): Acoustic emission studies on thermally and mechanically induced cracking in salt rock. In: Proc., 6th Conf. AE/MA in Geologic Structures and Materials. Trans. Tech. Publ., Clausthal-Zellerfeld, 245–265.

Martin, C. D., Chandler, N. A. (1994): The progressive fracture of Lac du Bonnet granite. Int. J. Rock Mech. Min. Sci. Geomech. Abstr. 31 (6), 643–659.

Matsuki, K., Kojima, T. (1995): A mechanism of stress memory in core-based methods for measuring in situ stresses. In: Proc., 8th Int. Congr. on Rock Mechanics vol. 1. Balkema, Rotterdam, 149–152.

Momayez, M., Hassani, F. (1998): A study into the effect of confining stress on Kaiser effect. In: Proc., 6th Conf. AE/MA in Geologic Structures and Materials. Trans. Tech. Publ., Clausthal-Zellerfeld, 187–194.

Nag, D. K., Seto, M., Vutukuri, V. S. (1996): Application of acoustic emission technique in estimating in situ vertical stress from borehole core rock sample. In: Trends in NDE Science & Technology. Proc., 14th World Conf. Non-Destructive Testing, vol. 4, Ashgate Publishing Comp., New Delhi. 2447–2450.

Nemat-Nasser, S., Horii, H. (1982): Compression-induced nonplanar crack extension with application to splitting, exfoliation, and rockbursts. J. Geoph. Res. 87 (B8), 6805–6821.

Oxenkrug, E. S., Tavostin, M. N., Filimonov, Yu. L., Shafarenko, E. M., Voznesensky, A. S. (1996): Use of acoustic emission method for the decision of the stability problem of the system "salt–cement–pipe" at underground gas and oil storage operations. In: Proc., 5th Session of the Russian Acoustical Society (in English). Moscow, 163–166.

Panasiyan, L. L., Kolegov, S. A., Morgunov, A. N. (1990): Stress memory studies in rock by means of acoustic emission. In: Proc., Int. Conf. Mech. Jointed and Faulted Rock. Balkema, Rotterdam, 435–439.

Rummel, F. (1965): Geräuschmessungen zur Untersuchung der Verformungsvorgänge in Gesteinsproben bei einachsiger Belastung. Gesellschaft für angewandte Geophysik mbH. Technische Mitteilung. Gebirgsmechanik I(1), 50–58 (in German).

Seto, M., Vutukuri, V. S., Nag, D. K. (1997): Possibility of estimating in situ stress of virgin coal field using acoustic emission technique. In: Rock Stress. Proc., Int. Symp. on Rock Stress. Balkema, Rotterdam, 463–468.

Shkuratnik, V. L., Lavrov, A. V. (1995): Memory effects in rock. J. Min. Sci. 31 (1), 20–28.

Shkuratnik, V. L., Lavrov, A. V. (1997a): Memory effects in rocks: physical features and theoretical models. Academy of Mining Sciences Press, Moscow (in Russian).

Shkuratnik, V. L., Lavrov, A. V. (1997b): Dreidimensionale Computersimulation des Kaiser-Effektes von Gesteinsproben bei triaxialer Belastung. Glückauf-Forschungshefte 58 (2), 78–81.

Spies, Th., Eisenblätter, J. (1998): Crack detection in salt rock and implications for the geomechanical situation. In: Proc., 3rd Int. Conf. Mech. Jointed and Faulted Rock. Balkema, Rotterdam, 405–410.

Utagawa, M., Seto, M., Katsuyama, K. (1997): Determination of in situ stress using DRA and AE techniques. In: Rock Stress. Proc., Int. Symp. on Rock Stress. Balkema, Rotterdam, 187–192.

Voznesensky, A. S., Demtchishin, Yu. V. (2000): AE signal computer processing at the gas storage cavern development. In: Geoecology and Computers. Proc., 3rd Int. Conf. on Advances of Computer Methods in Geotechnical and Geoenvironmental Engineering. Balkema, Rotterdam, 377–382.

Voznesensky, A. S., Oxenkrug, E. S., Tavostin, M. N., Filimonov, Yu. L., Shafarenko, E. M., Voznesensky, V. A. (1996): Acoustic emission in salt at the fading and stationary creep stages. In: Proc., 5th Session of the Russian Acoustical Society, (in English), Moscow, 133–136.

Yamamoto, K., Kuwahara, Y., Kato, N., Hirasawa, T. (1990): Deformation rate analysis: a new method for in situ stress estimation from inelastic deformation of rock samples under uni-axial compressions. Tohoku Geoph. J. (Sci. Rep. Tohoku Univ., Ser. 5) 33 (2), 127–147.

Yamamoto, K., Yabe, Y., Yamamoto, H. (1997): Relation of in situ stress field to seismic activity as inferred from the stresses measured on core samples. In: Rock Stress. Proc., Int. Symp. on Rock Stress. Balkema, Rotterdam, 463–468.

Yamshchikov, V. S., Shkuratnik, V. L., Lavrov, A. V. (1994): Memory effects in rocks (review). J. Min. Sci. 30 (5), 463–473.

Zhang, B., Li, H., Li, F., Shin, K. (1998): Kaiser effect tests on orientated rock core. In: Proc., 6th Conf. AE/MA in Geologic Structures and Materials. Trans. Tech. Publ., Clausthal-Zellerfeld, 211–224.

Authors' address: Dr. Alexander V. Lavrov, Catholic University of Leuven, Faculty of Applied Sciences, Department of Civil Engineering, Kasteelpark Arenberg 40, B-3001 Leuven, Belgium.